

## Identification of Ti-Anomaly in Stream Sediment Geochemistry using Stepwise Factor Analysis and Multifractal Model in Delijan District, Iran

Feridon Ghadimi<sup>1</sup>, Mohammad Ghomi<sup>1,2\*</sup>, Mojtaba Aref Sedigh<sup>1</sup>

*1- Department of mining Engineering, Arak University of Technology, Arak, Iran.*

*2- Department of Mining and Metallurgical Engineering, Amirkabir University of Technology, Tehran, Iran.*

*Received 03 Nov 2015; received in revised form 27 Apr 2016; accepted 30 Apr 2016*

*\*Corresponding author: mghomi@aut.ac.ir*

### Abstract

In this study, 115 samples taken from the stream sediments were analyzed to determine the concentrations of As, Co, Cr, Cu, Ni, Pb, W, Zn, Au, Ba, Fe, Mn, Sr, Ti, U, V and Zr. In order to outline mineralization-derived stream sediments, various mapping techniques including fuzzy factor score, geochemical halos and fractal model were used. Based on these models, concentrations of Co, Cr, Ni, Zn, Ba, Fe, Mn, Ti, U, V and Zr showed anomalies which are distributed over the andesitic volcanic rocks. In addition, an anomaly map for each element also ascertained the most ideal results for the exploration of deposits. Anomaly element associations can be successfully used in future geochemical exploration projects. According to the stream sediment study, it characterized a high Ti anomaly in central and northern parts of the area which was confirmed by heavy mineral study in sediments and litho-geochemical study in the andesitic unites.

**Keywords:** *Delijan, Multifractal Model, Stepwise Factor Analysis, Ti anomaly*

### 1. Introduction

The Urumieh-Dokhtar magmatic arc in Iran is a world-class Cu metallogenic belt. Porphyry, hydrothermal veins and magmatic and volcanic deposits of Cu, Pb, Zn, Au and other metallic and non-metallic elements widely occur in this belt [1-3]. Integration of stream sediment geochemical data with other types of mineral exploration data is a challenging issue that needs careful analysis of multi-element geochemical anomalies. Analysis of stream sediment samples can reveal various geochemical anomalies, some of which

can be considered as surficial geochemical signature of the deposit-type. Multivariate data analysis (e.g., factor analysis, cluster analysis and correlation analysis), and multifractal models have been successfully used to analyze geochemical data. Carranza [4] mapped anomalies in stream sediment using the mean+2SDEV (standard deviation), median+2MAD (median absolute deviation) and concentration–area (C–A) fractal methods of identifying threshold values in a geochemical data set. Carranza [5] determined

catchment basin modeling of stream sediment anomalies based on fractal analysis and revisits catchment basin modeling of stream sediment geochemical anomalies with regard to standardization of uni-element residuals derived from analysis of a number of subsets of stream sediment geochemical data in order to obtain a single set of uni-element residuals for classification of anomalies. Cheng et al. [6] showed principal component analysis (PCA) is frequently used in geosciences for information extraction. In many applications, masking PCA has been used to create subsets of samples or sub-areas to enhance the effect of the main objects of interest. Grunsky [7] showed that modern methods of evaluating data for associations, structures and patterns are grouped under the term 'data mining'. Mining data includes the application of multivariate data analysis and statistical techniques, combined with geographical information systems, and can significantly assist the task of data interpretation and subsequent model building. Zuo et al. [8] used hybrid method combining multivariate fuzzy comprehensive evaluation with asymmetric fuzzy relation analysis to map porphyry-copper prospectivity in the Gangdese district, Tibet, western China. Zuo et al. [9] applied singularity mapping technique to identification local anomalies using stream sediment geochemical data. They illustrated that weak anomalies are hidden within the strong variance of background and are not well identified by means of inverse distance weighted; neither are they clearly identified by the C–A method if this method is applied to the whole study area. Zuo [10] used robust neighborhood statistics, such as median, median absolute deviation (MAD) were used to model spatial variations of geochemical landscapes and to recognize weak geochemical anomalies in covered terrain by means of a case study from the Chaobuleng Fe polymetallic district covered by grassland, in Inner Mongolia (China).

Multivariate analyses are especially useful for this purpose because the relative importance of combinations of geochemical variables can be evaluated. There are many studies in the literature

that have used multivariate methods to analysis the geochemical exploration data [11, 9]. Factor analysis, one of the multivariate analysis methods, has been widely used for interpretation of stream sediment geochemical data [12-15]. The principal aim of factor analysis is to explain the variations in a multivariate data set by as few factors as possible and to detect hidden multivariate data structures [16]. Thus,, factor analysis is theoretically suitable for analysis of the variability inherent in a geochemical data set with many analyzed elements. Consequently, factor analysis is often applied as a tool for exploratory data analysis. Multivariate data analyses based on the frequency distributions or on correlations of geochemical data may be effective tools for solving some problems in the frequency domain, but are of limited use in the spatial domain due to spatial autocorrelation inherent in geochemical data. Fractal and multifractal models (specifically Concentration–Area) (C–A) proposed by Cheng et al. [17], involve both the frequency distributions and the spatial self-similar properties of geochemical variables and have been demonstrated to be effective tools for decomposing complex and mixed geochemical populations and to identify weak geochemical anomalies hidden within strong geochemical background. Cheng [18] applied local singularity for mapping anomalies based on multifractal theory. It assembles geochemical map at different scales and calculates an index indicating the scaling characteristics of enrichment and depletion of geochemical concentration at multiple scales. Cheng and Agterberg [19] proposed a new local singularity mapping method for assembling element concentration values from stream sediment samples to delineate anomalous areas induced by buried mineral deposits, which are often missed in ordinary geochemical surveys and mapping. Cheng et al. [20] introduced a fractal filtering technique newly developed on the basis of a spectral energy density vs. area power-law model in the context of multifractal theory. It can be used to map anisotropic singularities of geochemical landscapes created from geochemical concentration values in various surface media such as soils, stream sediments, tills and water.

Zuo [21] applied the spectrum-area technique to Gangdese belt based on stream sediment data. Zuo and Xia [22] used fractal and multifractal methods to map the local anomalies. The spectrum-area model (S-A) method was used to separate the anomaly from the singularity map. Hassanpour and Afzal [23] proposed concentration-number (C-N) multifractal modeling for geochemical anomaly separation in Haftcheshmeh porphyry system. Heidari et al. [24] used the Concentration–Area (C–A) fractal method and separated mineralization phases based on surface litho-geochemical Au, Ag, As and Cu data. Afzal et al. [25] determined geochemical anomalies using power spectrum–area (S–A) method based on the grade values of Cu, Mo and Au in soil samples.

In this paper, integrating method, factor and cluster analysis and concentration-area fractal model are used to identify geochemical anomalies based on stream sediment geochemical data from the Delijan region. Geochemical analyses of 115 stream sediment samples for 17 elements including As, Co, Cr, Cu, Ni, Pb, W, Zn, Au, Ba, Fe, Mn, Sr, Ti, U, V and Zr, collected by the Geological Survey of Iran (GSI) from Delijan area (Central Iran) has been used to test the proposed approach using stepwise factor score. In all geochemical data distribution maps described in this paper, the cumulative percentile equivalent to 97.5% frequency has been considered as a reference value/threshold to evaluate and compare the efficiency of the discussed methods.

## 2. Geological setting

The Delijan area is situated in Markazi Province in Central Iran located in the main Iranian Cenozoic Urumieh-Dokhtar magmatic belt [26]. This belt extends from NW to SE which hosts the large Iranian porphyry deposits [1]. The study area is mainly comprised of Cenozoic rocks, which were intruded by granodioritic intrusions rocks (Fig. 1). These rocks are including marl, sandstone, Eocene andesitic tuff and lava and Oligo-Miocene limestone, marl of Qom formation. Magmatic events in Delijan area happened as intrusive and dikes with granodioritic and diabase affinities, respectively. The main structural feature has a NE–SW trending. Moreover, the main alteration zones of epidotization and chloritization types were

decompose a mixed pattern of arsenic in accompanied by the vein fillings of Fe-oxides. Mineralization has occurred into the andesitic dikes and in host rocks such as andesitic tuff and andesitic lava. The ore minerals, i.e. hematite, magnetite, Ti-magnetite, ilmenite and barite are present and occur in the host rocks [27]. The source of mineralization at the Delijan area is interpreted as magmatic events. Petrography studies show that the area is composed of pyroclastic, volcanic and intrusive rocks. Basaltic andesite lava consisted of plagioclase, pyroxene, and hornblende minerals (Fig. 2). These rocks are aphanitic and devitrified. Andesite has been altered to chlorite, epidote and sericite. Andesitic tuff included vitric and detrital texture and has plagioclase, hornblende minerals and rock fragments. We can see sericite and chlorite alteration in these rocks. Andesitic dikes are other forms of magma in this area that have porphyritic texture and plagioclase, hornblende, pyroxene are abundant minerals, and epidote is the secondary mineral in these rocks. This area has a small granodiorite body that has granular texture and minerals such as quartz, plagioclase and feldspar are the main rock forming minerals.

## 3. Materials and methods

### 3.1. Stream sediments and sample collection

One of the most commonly used methods in geochemical prospecting is the study of active stream sediments. According to the definition given by the Forum of the European Geological Surveys (FOREGS), these are represented by the fine and medium size fraction of sediments carried and settled by second order streams. Stream sediments can be considered as averagely representative of the outcropping rocks in the drainage basin, upstream of the sampling point [28] (Fig.3). The Extended Sample Catchment Basin (ESCB) mapping technique, discussed in this paper, can be used to display the spatial distribution of geochemical variables measured in stream sediments. [29,30]. This approach is based on the allocation of an area of statistical representativeness to each sample, and the concentration measured in the stream sediments can be considered as the average reference values for this area. ESCBs can be easily identified considering the position of the sampling points within the hydrographic network and using the confluences between the streams of highest rank as break points for representing the geochemical background changes. The area of each sample was

determined on geographical information system (GIS). Over a total basin surface of about 1773 km<sup>2</sup>, 115 stream sediment samples (150 μm particle size diameter) were collected with an average sampling density of 1 sample/15.50 km<sup>2</sup> (Fig. 3). The concentration of 17 chemical

elements including As, Co, Cr, Cu, Ni, Pb, W, Zn, Au, Ba, Fe, Mn, Sr, Ti, U, V and Zr was measured by ICP-MS method. Afterwards, ESCB mapping, was tested and compared using GIS functions of spatial analysis.

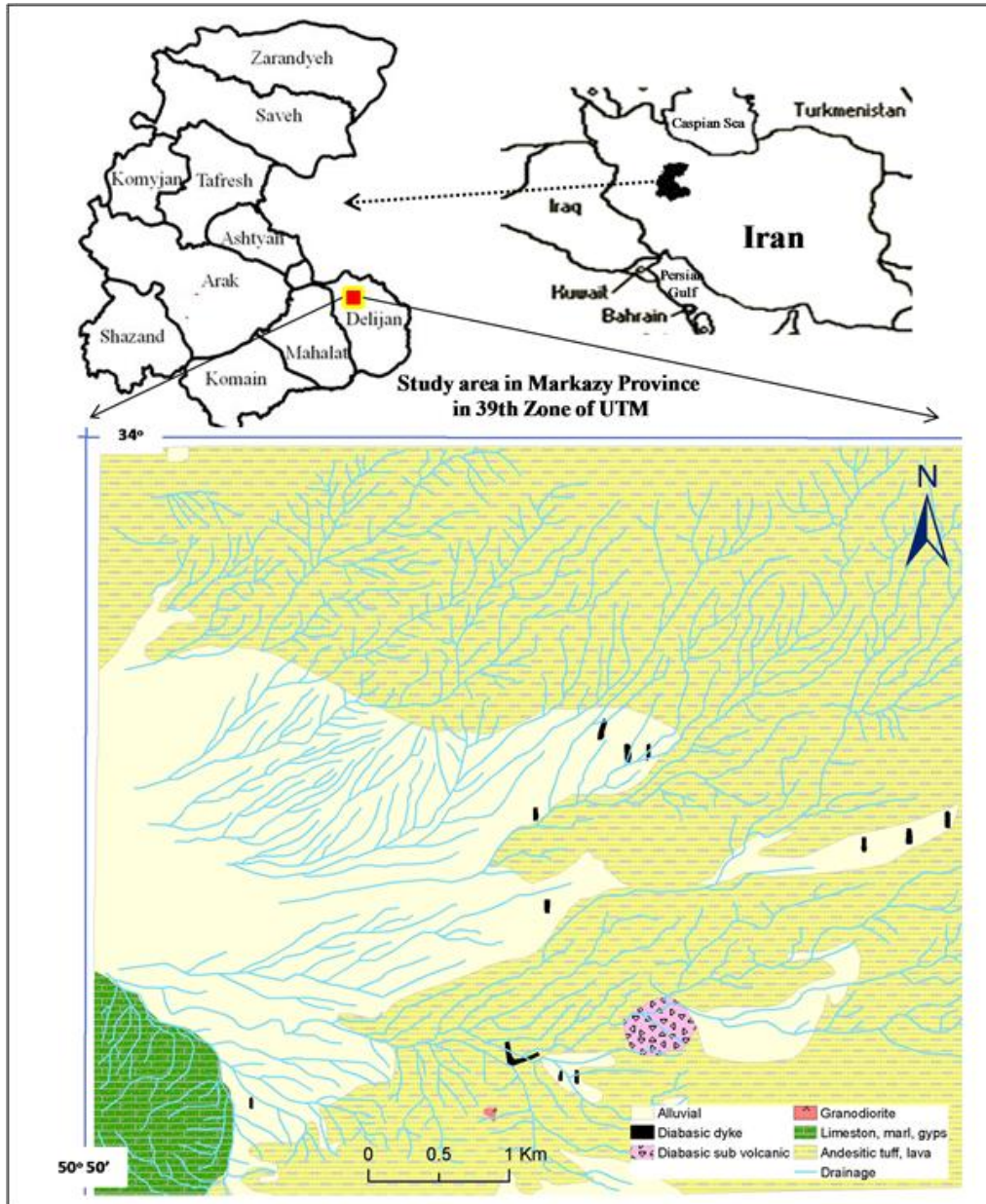


Fig.1. Location of study area in Iran and simplified geological map in Delijan.

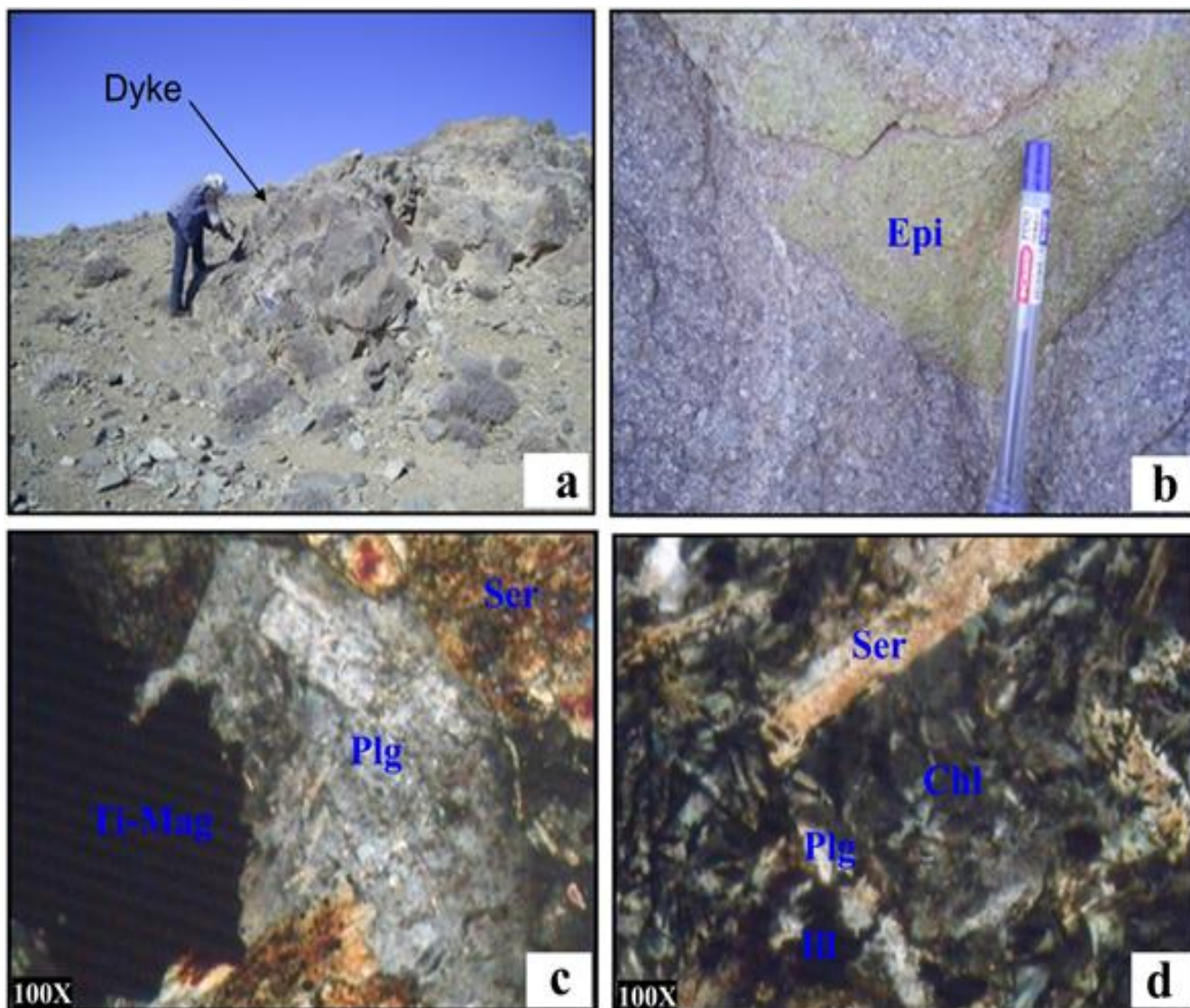


Fig.2. Photographs of representative samples; (a) andesitic dike; (b) Epidite (Epi) alteration in the andesite; (c,d) microphotographs of andesite rock that plagioclase (Plg) and mafic minerals are effected by sericitization (Ser) and chloritization (Chl) alteration and Opaque minerals such as: Ti-magnetite(Ti-Mag), Illmenite (Ill).

### 3.2. Data analysis

A total of 17 variables from 115 stream sediment data were used in our analysis. Since these variables are not symmetrically distributed (especially As, Cr, Au, Ba and U), we examined the normality of each variable based on skewness, and if a variable does not satisfy the provision, the variables were transformed [31]. In our data set, none of the variables passed this normality distribution. Therefore, isometric logratio-transformations were conducted for the skewed variables to achieve normality transformation [32-34]. Isometric logratio (ilr) transformations are of useful classes of logratio transformations with good theoretical properties. In addition to data transformation, all variable were standardized [33, 34].

In order to determine the relationships between the elements and groups, stepwise multivariate analysis was employed. Results of the analyses were evaluated with the STATISTICA program. The factor analysis method was carried out based on the examination of dependency among the artificial variables which are computed from covariance and correlation coefficient matrixes [35]. In other words, eigenvalues and eigenvectors of covariance and correlation coefficient matrixes are interpreted. Also, varimax rotation was performed to strengthen the factor loads. Cluster analysis (hierarchical cluster analysis) was carried out using Ward's method and Pearson's correlation coefficients and the results are given in a dendrogram.

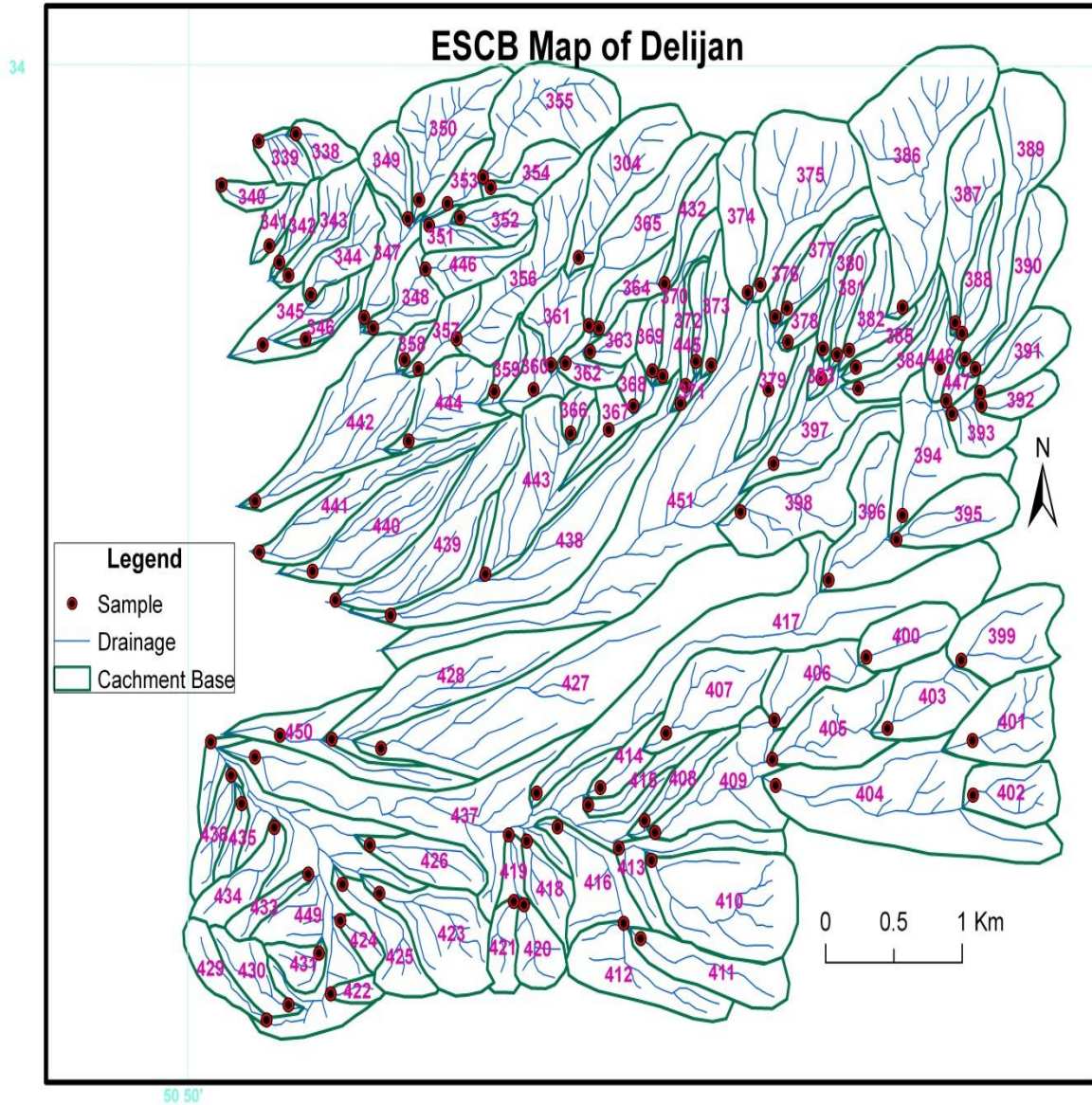


Fig.3. Use of ESCB technique in the Delijan district.

Fractal models may be similarly applied to separate populations, but generally do not require specific distribution types to be specified. In the C-A model, the spatial distribution of observations is taken into account [36-39]. If  $A(\rho)$  is the area of concentration value greater than  $\rho$  in a contour map of spatial data, then  $A(\rho)$  should be a decreasing function versus  $\rho$ . If  $v$  represents a threshold value, the following Eq. 1, can be experimentally fitted to the data:

$$A(\rho \leq v) \propto \rho^{-\alpha_1}; A(\rho > v) \propto \rho^{-\alpha_2} \quad (1)$$

where  $v$  represents a concentration contour (or threshold) and  $A(\rho)$  denotes area enclosed by concentration values ( $\rho$ ) that are  $\leq v$  or  $> v$ ;  $\alpha_1$  and

$\alpha_2$  are fractal dimensions of the data distributions that can be estimated from the slopes of straight lines fitted to the log-log plot of  $A(\rho)$  versus  $\rho$ ;  $\propto$  denotes proportionality. If a plot of  $A(\geq \rho)$  versus  $r$  (in log-log plot) is linear then all data belong to a single population and the distribution is a simple fractal. If, however, the plots can be fitted with several straight-line segments, then the distribution is multi-fractal and the break-points between straight-line segments are the thresholds which separate the populations. The greater the difference between fractal dimensions, the clearer is the separation between populations [40].

#### 4. Results and discussion

##### 4.1. Elemental concentrations of stream sediments

Descriptive statistics such as minimum, median, maximum and percentiles (25, and 75%) for 17 elements used in this study are shown in Fig.4. Most of the elements have a wide range of variations of several magnitudes. This was evident for As, whose concentrations vary from 6.50 ppm to 13 ppm with a median of 10 ppm. Similar variability was also found for other elements. The mean Co content in the sediments is 15 ppm, ranging from 9 to 30 ppm (Fig. 4). The Cr concentrations in the sediment samples vary from 63 to 153 ppm and the average is 108 ppm. Copper content in the sediments varies from 10 to 108 ppm with an average of 24 ppm. Nickel concentration in sediments is between 15 and 45 ppm with an average of 27 ppm. The minimum Pb concentration in the sediments is 10 ppm and the maximum value is 50 ppm. The average Pb concentration is 11 ppm. The mean W content in the sediments is 1.28 ppm, ranging from 1.00 to 3.00 ppm. The Zn concentration in sediments varies from 24 to 103 ppm and an average is 48 ppm. Gold content in the sediments varies from 0.001 to 0.003 ppm with an average of 0.002 ppm. Barium content in the sediments varies from 172

to 337 ppm with an average of 250 ppm. The minimum Fe concentration in Delijan sediments is 3% and the maximum value is 10 %. The average Fe concentration is 5.06%. The mean Mn content in the sediments is 690 ppm, ranging from 397 to 1355 ppm. The mean Sr content in the sediments is 262 ppm, ranging from 137 to 5330 ppm. Titanium concentration in sediments is between 3059 and 15119 ppm with an average of 5705 ppm. The mean W content in the sediments is 1.28 ppm, ranging from 1.00 to 3.00 ppm. The U concentrations in sediments vary from 1.00 to 7.00 ppm and an average is 3.29 ppm. The minimum V concentration in Delijan sediments is 84 ppm and the maximum value is 463 ppm. The average V concentration is 176 ppm. The Zr concentration in sediments varies from 71 to 140 ppm and an average is 98 ppm. The concentrations of elements in stream sediments of the study area were compared with the values of the upper continental crust. The elements mean such as As, Cr, Ti, U and V exhibit depletion relative to the upper continental crust based on Wedepohi [41] and Rudnick and Gao [42]. Maximum values for all of the elements present high values relative to the upper continental crust. Therefore, there are many stream sediments that have high elemental values.

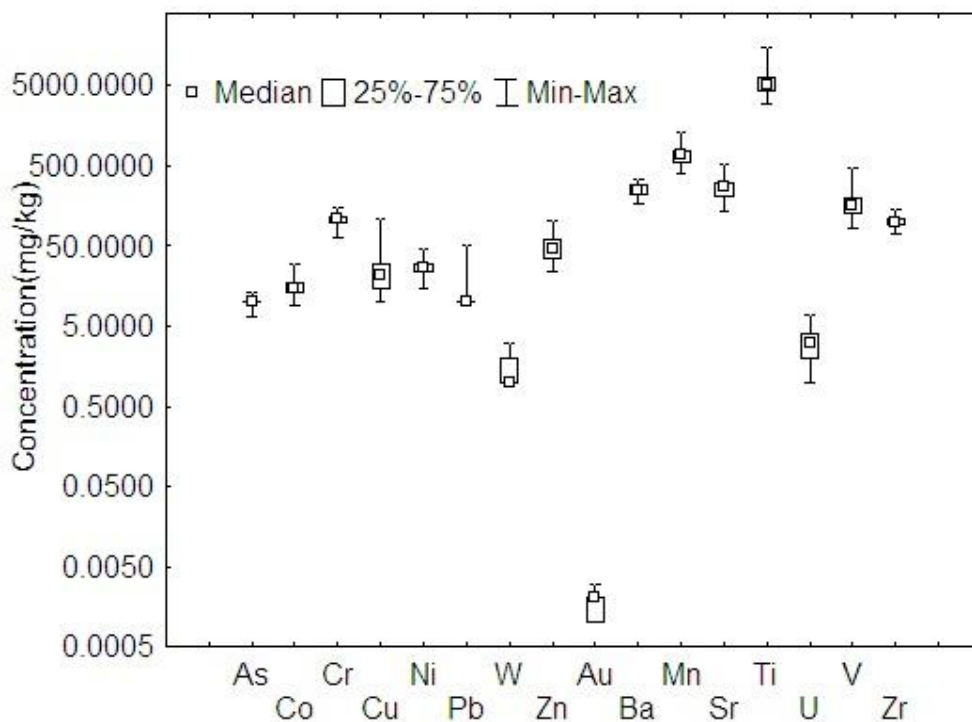


Fig.4. Elemental concentrations of stream sediments of Delijan district (except Fe is %).

## 4.2. Statistical analysis

The principal component analysis has been used for extraction of factors. Furthermore, it applied varimax rotation of factors [43], and then used a three-step factor analysis to extract components representing anomaly [13]. In the first step, factor analysis has yielded six rotated components, each with eigenvalues greater than 1 (Table 1). Six significant factors have produced, that explain 76.60% of the variance of the original data set (Table 1).

Most of the variance is contained in the factor 1 (34.05%) in the original data set, which is associated with the component Co, Fe, Ti and V (Table 1). Factor 2 explains 14.78% of the variance and is mainly related to elements Zn, Ba, Mn and Zr. The As contributes most strongly to the third factor that explains 8.40% of the total variance. The fourth factor is concerned with Cr and Ni and represents 7.23% of the total variance. Factor 5 explains 6.24% of the variance and is mainly related to elements Au and Sr. Using the stepwise factor analysis, the number of factors can be reduced and the anomaly intensity can be increased. The sixth factor is concerned with U and represents 5.89% of the total variance. Increasing anomaly's intensity means that the number of adjacent anomalous samples in sediments has increased with respect to the total number of anomalous samples in the study area. Regarding this, the data for Cu, Pb, W and Sr which have weak correlations were omitted for all factors. Then, the results of the second factor analysis for the remaining geochemical data were used to calculate factor scores for each sample. Table 2 provides the rotated factor matrix and the factor plot in rotated space for the second factor

analysis. Factor 1 represents Co, Fe, Ti and V association, factor 2 related to Zn, Ba, Mn and Zr, factor 3 and factor 4 shows Ni, Cr and U, respectively. For step 3, we omitted As and Au and total variance changed from 74.00% to 85.72% (Table 3). There are not any changes in the amounts of factors and variables in step 3, but the total variance increased and we stop stepwise factor analysis in this step (Fig.5). According to Tables 1 and 3, the total variance relevant to factor 1, has increased from 34.05% in the first factor analysis up to 48.24% in the second one. Consequently, through stepwise factor analysis whereby poor indicator elements are removed from the data and the total variance related to each factor increased. In order to reveal the relationship between elements and element groups in the first and third factor analyses, other multivariate analysis techniques such as cluster analysis and correlation matrix were performed (Table 4). Cluster analysis (hierarchical cluster analysis) was carried out using Ward's method and Pearson's correlation coefficients and the results are provided in a dendrogram (Figs. 6 and 7). Results of cluster analysis in step 1 indicate that the elements comprise several groups that are mainly similar to the first stepwise of the factor analysis (Fig.7). In the third step of cluster analysis, all clusters are corresponding to the third stepwise factor analysis and there are four groups (Fig.7). The first group is including Ti, V, Fe and Co; the second groups consists of Zr, Ba, Mn and Zn; the third group composed Ni and Cr; and the fourth group included U. All groups coincide with the results of factor analysis and correlation coefficients in correlation analysis in the third stepwise (Tables 2, 3 and 4).

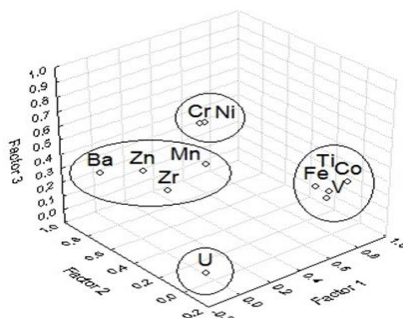


Fig.5. Factor plot in rotated space in the third step of factor analysis.

**Table 1. Rotated factor analysis in first step (loadings in bold represent the selected factors based on threshold of 0.70).**

	Factor 1	Factor 2	Factor 3	Factor 4	Factor 5	Factor 6
As	-0.01	-0.03	<b>0.84</b>	0.07	-0.15	-0.03
Co	<b>0.91</b>	0.03	-0.04	0.20	-0.04	0.11
Cr	0.04	0.25	-0.01	<b>0.82</b>	0.06	-0.01
Cu	0.36	0.40	-0.49	0.31	-0.03	0.33
Ni	0.17	0.25	0.19	<b>0.77</b>	0.13	0.01
Pb	-0.35	0.39	0.24	-0.45	0.33	-0.12
W	0.01	0.17	0.45	0.06	0.19	0.03
Zn	0.29	<b>0.82</b>	0.23	0.12	0.22	0.04
Au	0.27	-0.06	-0.05	0.05	<b>0.72</b>	0.21
Ba	0.01	<b>0.88</b>	0.04	0.23	0.01	0.11
Fe	<b>0.92</b>	0.25	-0.04	0.06	-0.08	0.07
Mn	0.51	<b>0.67</b>	0.15	0.14	0.09	0.04
Sr	-0.27	0.16	0.09	0.11	0.53	-0.26
Ti	<b>0.93</b>	0.12	-0.03	0.08	0.11	-0.10
U	-0.03	-0.03	0.01	-0.01	-0.01	<b>-0.92</b>
V	<b>0.96</b>	0.16	-0.02	0.01	0.03	0.06
Zr	0.27	<b>0.71</b>	-0.18	0.16	-0.11	-0.16
Eigenvalue	5.78	2.51	1.42	1.22	1.06	1.01
% Total - variance	34.05	14.78	8.40	7.23	6.24	5.89
Cumulative - %	34.05	48.83	57.23	64.47	70.71	76.60

**Table 2. Rotated factor analysis in second step of factor analysis (loadings in bold represent the selected factors based on threshold of 0.70).**

	Factor 1	Factor 2	Factor 3	Factor 4
As	-0.03	-0.11	0.54	-0.43
Co	<b>0.92</b>	0.06	0.15	0.14
Cr	0.03	0.33	<b>0.73</b>	0.15
Ni	0.15	0.31	<b>0.77</b>	0.06
Zn	0.25	<b>0.83</b>	0.21	0.03
Au	0.25	-0.07	0.29	0.40
Ba	-0.03	<b>0.89</b>	0.18	0.08
Fe	<b>0.92</b>	0.27	0.04	0.04
Mn	0.57	<b>0.72</b>	0.16	0.04
Ti	<b>0.93</b>	0.17	0.05	0.01
U	-0.01	-0.02	0.01	<b>-0.83</b>
V	<b>0.95</b>	0.19	0.01	0.07
Zr	0.24	<b>0.72</b>	0.03	-0.09
Eigenvalue	5.37	2.08	1.09	1.07
% Total - variance	41.31	16.01	8.43	8.23
Cumulative - %	41.31	57.32	65.75	74.00

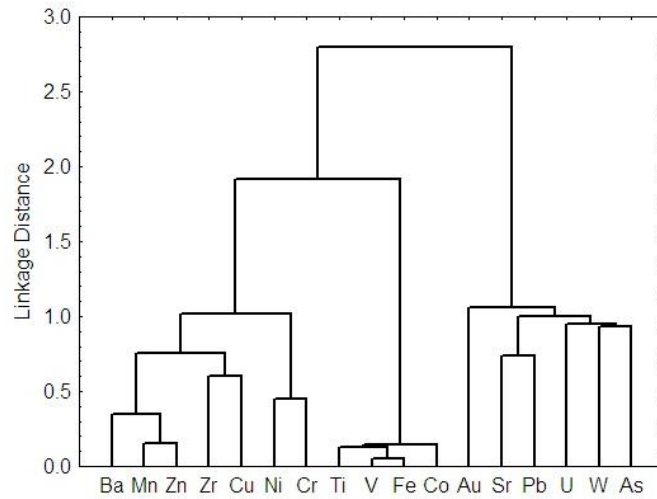


Fig.6. Dendrogram depicting the hierarchical clustering of the elements in the first step.

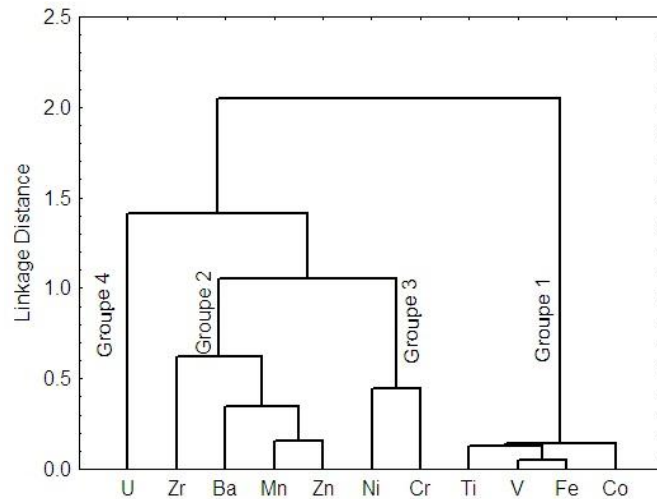


Fig.7. Dendrogram of the elements in the third step.

Table 3. Rotated factor analysis in third step of factor analysis (loadings in bold represent the selected factors based on a threshold of 0.70).

	Factor 1	Factor 2	Factor 3	Factor 4
Co	<b>0.93</b>	0.03	0.21	0.10
Cr	0.06	0.18	<b>0.87</b>	0.02
Ni	0.15	0.26	<b>0.81</b>	-0.01
Zn	0.24	<b>0.88</b>	0.16	0.09
Ba	-0.04	<b>0.86</b>	0.27	0.08
Fe	<b>0.92</b>	0.26	0.07	0.02
Mn	0.56	0.74	0.15	0.07
Ti	<b>0.93</b>	0.17	0.07	-0.07
U	-0.06	-0.02	-0.01	<b>-0.97</b>
V	<b>0.95</b>	0.21	-0.01	0.05
Zr	0.23	<b>0.71</b>	0.12	-0.20
Eigenvalue	5.31	2.05	1.04	1.03
% Total - variance	48.24	18.63	9.44	9.41
Cumulative - %	48.24	66.87	76.32	85.72

**Table 4. Pearson correlation coefficient matrix for elements in the third step ( $p \leq 0.01$ ).**

	Co	Cr	Ni	Zn	Ba	Fe	Mn	Ti	U	V	Zr
Co	1.00										
Cr	0.21	1.00									
Ni	0.35	0.55	1.00								
Zn	0.28	0.27	0.47	1.00							
Ba	0.07	0.43	0.36	0.74	1.00						
Fe	0.89	0.17	0.26	0.44	0.26	1.00					
Mn	0.58	0.30	0.41	0.84	0.65	0.68	1.00				
Ti	0.85	0.23	0.18	0.38	0.11	0.86	0.68	1.00			
U	-0.16	-0.04	-0.01	-0.09	-0.06	-0.09	-0.10	0.01	1.00		
V	0.88	0.10	0.21	0.44	0.15	0.95	0.68	0.91	-0.11	1.00	
Zr	0.27	0.27	0.29	0.52	0.46	0.39	0.52	0.33	0.05	0.33	1.00

Potential map was obtained by fuzzy factor score map (FFS). After the factor score (FS) of each sample, weights should be assigned to each sample to represent probability of the presence of the deposit-type upstream of the sample. The weights are here called the fuzzy factor score map (FFS: [8, 13]). In general factor analysis, the response variable is continuous and the values outside the [0, 1] range are inappropriate if the response variable relates to probability. In order to constrain the values of the predicted response variable within the unit interval [0, 1], Cox and Snell recommended use a logistic model in order to represent the probability [44], Eq. 2:

$$FFS = \frac{e^{FS}}{1+e^{FS}} \quad (2)$$

where FS is the factor score of each sample per indicator factor obtained in a factor analysis. The FFS is, therefore, a fuzzy weight of each stream sediment geochemical sample for each indicator factor. In this way, the weights of different classes of evidential maps are calculated based on the FFS of samples per indicator factor obtained in the stepwise factor analysis. Values of the FFS corresponding to cumulative content of 99.5%, 97.5%, 84%, 75%, 50%, 25% and minimum were determined for the indicator factors for mapping purposes. In this paper, distributions of FFS for

indicator factors are represented as interpolated values (Fig.8). A value of the FFS corresponding to cumulative percentile of 97.5% frequency was selected as the threshold value to separate anomalous and background samples, like in the FS distribution maps (Fig.8).

The map of the first fuzzy factor scores (FFS1: Fig.8) shows high values disposed in andesitic volcanic rocks in form of lava and dike and concentrated mainly in northwest parts of the study area which are the favorable areas for Ti, V, Fe and Co deposits. The first fuzzy factor scores represent mixed geochemical populations, because the Urumieh-Dokhtar belt has a complex geological structure of different tectonic zones and have different geochemical background and threshold ranges. The second and third fuzzy factor scores (FFS2, FFS3) represent the high-frequency anomalies. They are generally related to the andesitic lava rocks which are favorable area for Zr, Ba, Mn, Zn, Ni and Cr deposits. It occurred in the northern and southern parts of the study area. The fourth fuzzy factor scores (FFS4) map shows that high values occur in marl of Eocene age, which are favorable area for U deposits. These results indicate potential for the discovery of multi-element deposits which are mainly distributed in the andesitic volcanic rocks of Eocene age and have a similar origin.

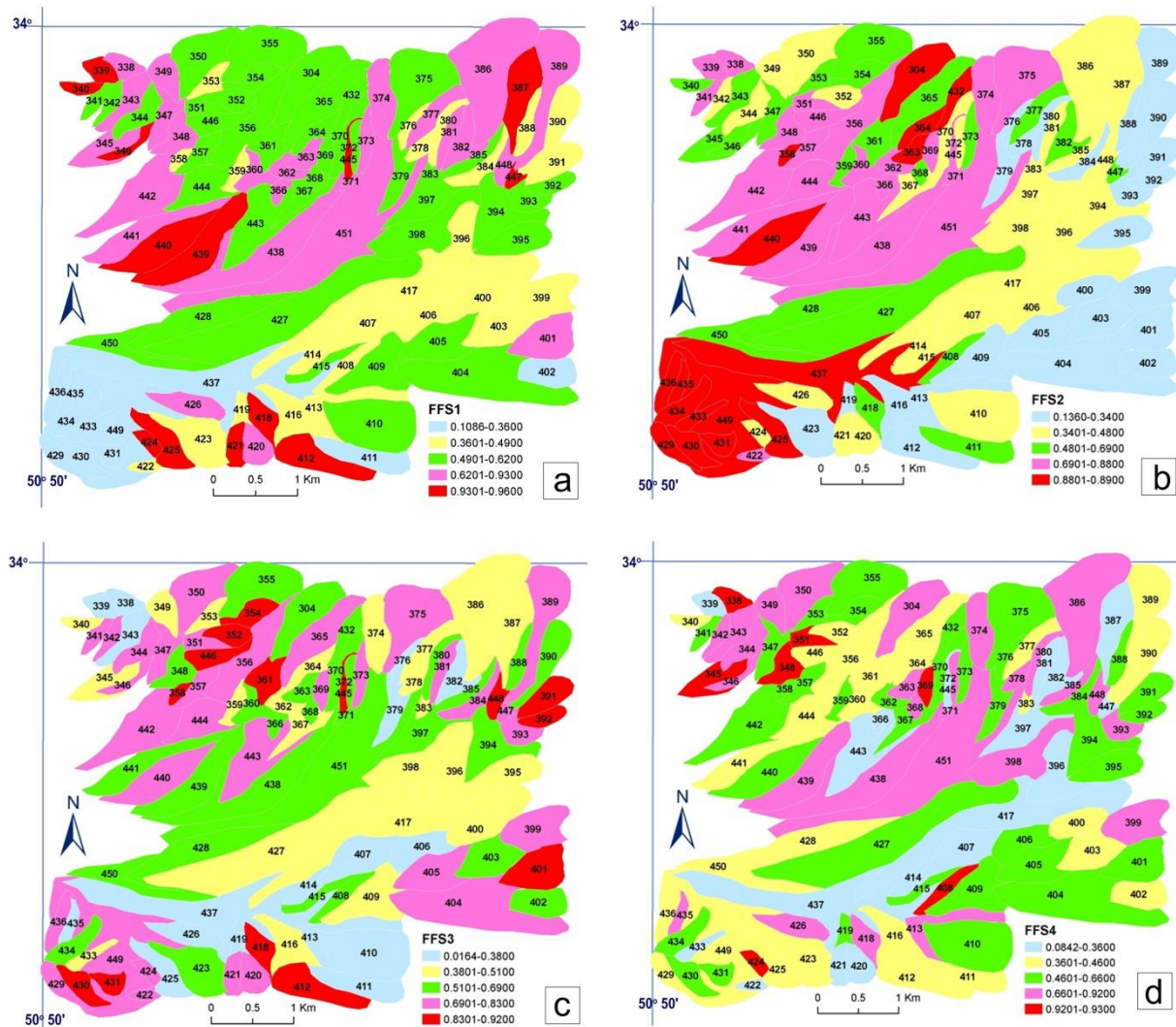


Fig.8. FFS distribution map for (a) FFS1 (Ti, V, Fe and Co); (b) FFS2 ( Zr, Ba, Mn and Zn) ;(c) FFS3 (Ni and Cr) and (d) FFS4 (U) indicator factor based on 99.5%, 97.5%, 84%, 75%, 50%, 25% and minimum contents.

### 4.3. Application of fractal modeling

Concentration–area relations in multifractal model were computed by assigning an area of influence to each sampled point and summing all elemental areas whose concentration lie below a given value [17, 29, 5]. This procedure was repeated for different elemental concentrations. Based on decreasing grades, the evaluated grades in catchments were sorted out and cumulative areas were calculated for grades [22, 40]. Finally, log–log plots were provided for Ti, V, Fe and Co (Fig. 9). On the basis of this procedure, there are several populations for Ti, V, Fe and Co respectively as shown in Fig. 9, but the best population were selected. As shown in Fig. 9, there are two break lines as a whole called background and anomaly. Anomaly break line is

divided into three parts of low anomaly, medium anomaly and high anomaly. Titanium anomaly threshold (high anomaly) is 5301 ppm based on log–log plot as depicted in Fig. 9.

Vanadium log–log plot shows that most of V enrichment occurred at 441 ppm. Iron anomaly threshold is about 8.1 %. Most of Co enrichment started from 27 ppm. The break between the straight-line segment and the corresponding values of above elements have been used as the cut-offs to reclassify catchment values in the interpolated maps [38]. The main maps are indicated in Fig. 10. Interpolated maps of the distribution of Ti, V, Fe and Co based on the modeled populations by the values equal to 99.5%, 97.5%, 84%, 75%, 50%, 25% and the

minimum cumulative contents are presented in Fig. 10.

A final main map value corresponding to high anomaly is used to generate the final distribution map for comparison with the main maps obtained from fractal method (Fig. 11). The anomaly map shows that high anomalous values occur in andesitic volcanic rocks of Eocene age in northern and southern parts of the study area. There are a few deposits in marl and limestone of Oligocene age and in granodiorite intrusive rocks. The multi-

element anomalies of above elements occurring in volcanic rocks should be further investigated in the next step of mineral resource exploration. However, investigation of heavy minerals exhibited that illmenite and Ti-magnetite minerals are abundant in stream sediments and in andesitic dikes [27]. Therefore, in the later studies, multi-element deposit in volcanic rocks and specially Ti deposit in alluvial deposit and rocks should be investigated.

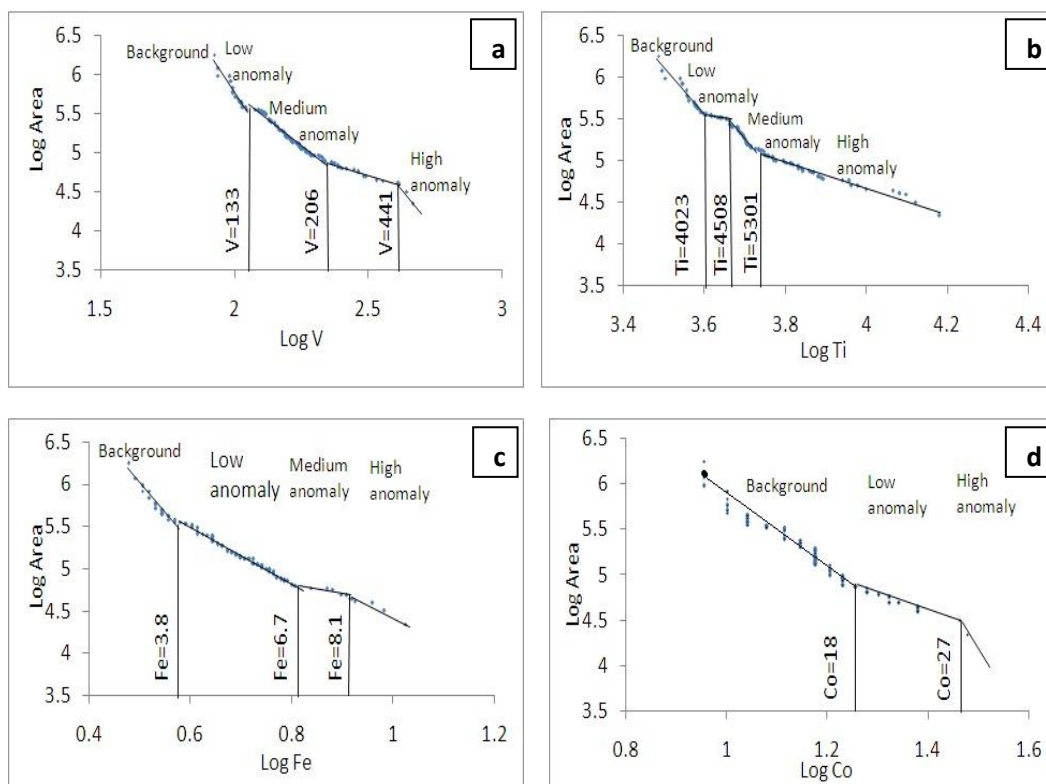
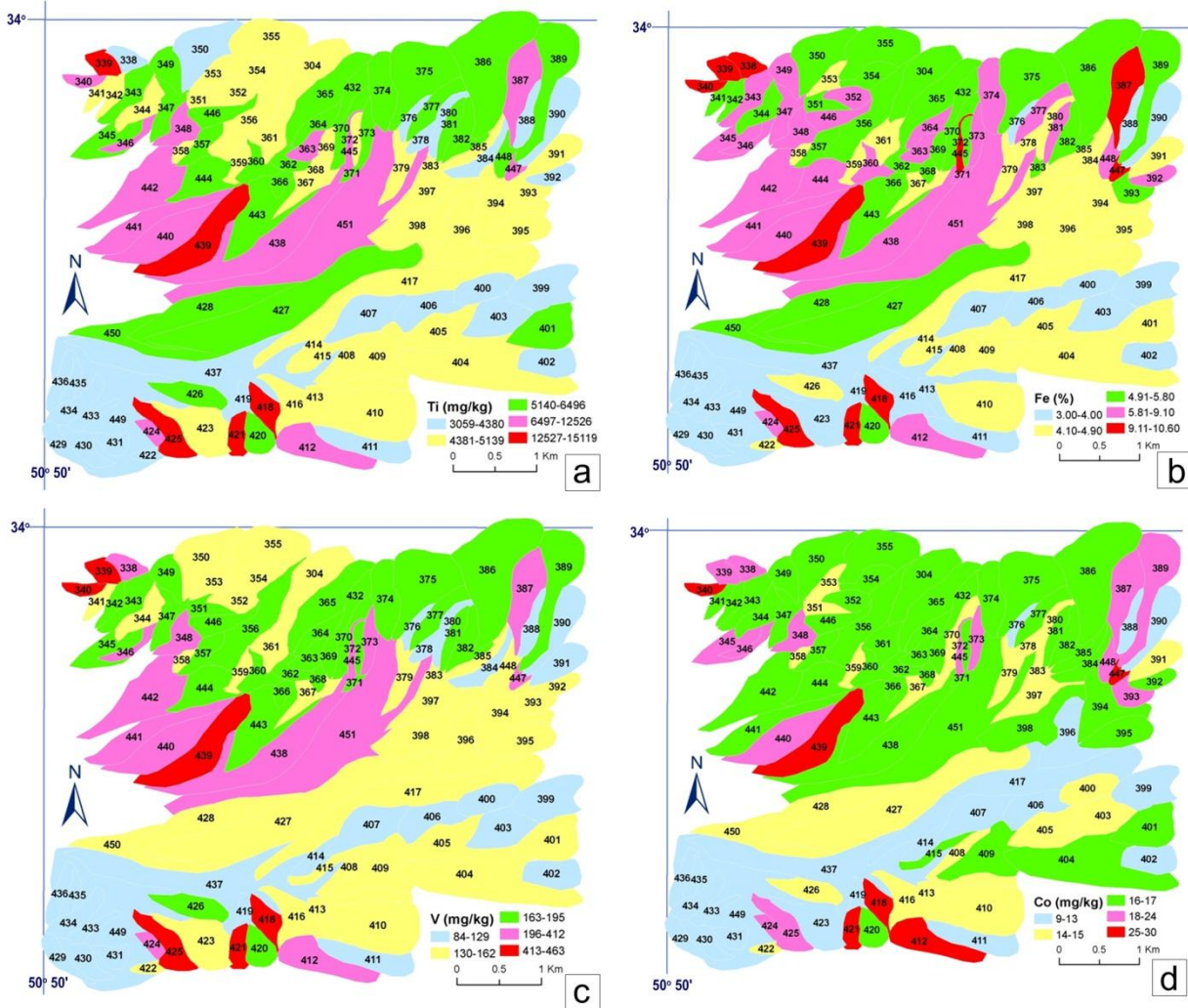


Fig.9. Log–log plots (concentration–area method) for elemental component; V (a), Ti (b), Fe (c), Co (d), concentration of elements is mg/kg, but Fe is %.

Geochemical halos can be ascertained more efficiently with a combination of two or more pathfinder elements rather than a single element [45, 46]. This practice is called ‘multielement halos technique’, where halos are slightly affected by the random errors. This technique increases the likelihood that the geochemical data are actually the geological features. Multielement halos technique is computed as Eq. 3:

$$GH = \left(\frac{X_1}{X_0} + \frac{Y_1}{Y_0}\right); \left(\frac{X_2}{X_0} + \frac{Y_2}{Y_0}\right); \dots \left(\frac{X_N}{X_0} + \frac{Y_N}{Y_0}\right) \quad (3)$$

where  $X_1, X_2, \dots, X_N$  are concentrations of X in samples 1, 2, ..., N;  $Y_1, Y_2, \dots, Y_N$  are concentrations of Y in samples 1, 2, ..., N; and  $X_0$  and  $Y_0$  are background values of X and Y elements. Median values are used as the background values for each element. Fig. 12 shows the anomaly halos of Ti and pathfinder elements in the Delijan area (GH1 and GH2). The anomaly halos of Ti and Fe-Co-V multi elements (GH1) are more than that of Ti and Fe (GH2) but have a similar form.



**Fig.10. Distribution map of elemental component; Ti (a), Fe (b), V (c) and Co (d), plotted based on 99.5%, 97.5%, 84%, 75%, 50%, 25% and minimum contents.**

Comparing different models such as fuzzy factor score (FFS-Ti), main concentration (Ti), fractal model (Fr-Ti) and geochemical halos (GH2-Ti) in Fig. 13, the main difference is that the target areas delineated based on the fact that the whole study area is mainly located in the northwest and south part of the study area. Significant spatial area by fuzzy factor score (FFS-Ti) method, main concentration (Ti) and geochemical halos occupy 13.0%, 12.5% and 10.5%, respectively. Fractal

model (Fr-Ti) occupies more than 50% of the total study area. The targets in Fig. 13 are nearly similar for the three above models but are different from fractal model (Fig.14). However, the target areas for Ti deposits in fractal method (Fr-Ti) are like that of average for upper continental crust (Ti). In overall, however, the fractal model could identify local anomalies as clearly as the other Ti mapping model.

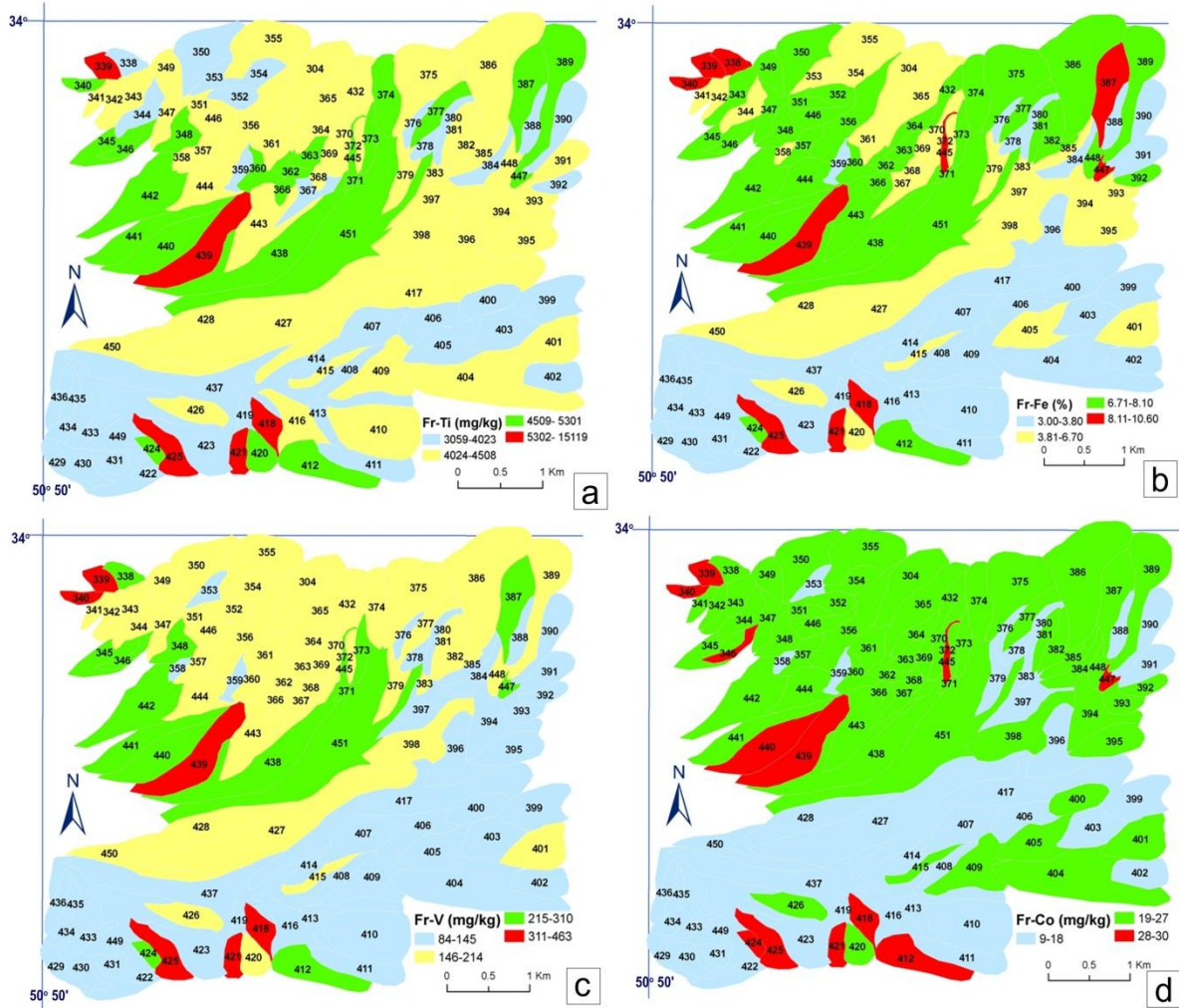


Fig.11. Distribution map of elemental components; Ti (a), Fe (b), V (c) and Co (d), plotted based on threshold of fractal model (Fr).

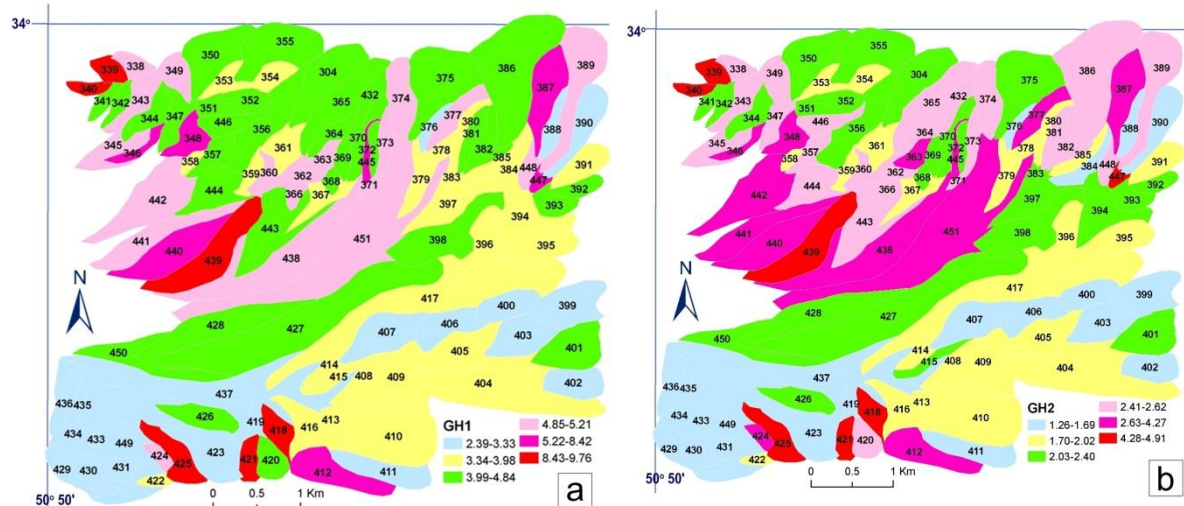


Fig.12. Geochemical halos for Ti and pathfinder elements such as (a); Fe, V and Co (GH1) and (b); Ti with Fe (GH2) based on 99.5%, 97.5%, 84%, 75%, 50%, 25% and minimum contents.

By using fractal model, two potentially prospective areas for Ti exploration were identified, i.e. the center and the north of the study area in which the andesitic units are

located. The presence of andesitic outcrop in these areas means that a high visible evidence of potential mineralization is present at the surface suggesting that the litho-geochemistry studies (in

addition to stream geochemistry) are useful tools for exploration within this area. There exists a very good correlation between the calculated anomalous threshold values and the range of concentrations obtained in the rocks, especially for Ti in the Delijan area. Such correlation is also valid by heavy minerals. These results also are interpreted according to their nature, especially multi fractal curves in log–log plots. Ti concentration in the area may be a result of the three steps of enrichment, i.e., mineralization and later dispersions. Major Ti mineralization occurred by the extrusion of Eocene andesitic lava and dikes in this area. The occurrence of high Ti enrichments in andesitic units in central and northern parts of the area has been actually realized in the samples collected from the field. High Ti intensive anomalies were found within

andesitic units. The chemical analysis of seven samples of in andesitic unites in lavas and dikes showed the value of Ti is 0.75 to 0.98 percent. All samples are rich of illmenite mineral in the ore microscopic studies. Study of 10 heavy mineral samples also, identified the presence of illmenite in the central and northern parts of the area. Statistical analysis of stream sediment also confirms these results. Further, geological evidences include lithological information, proved that accuracy of the results is obtained from different models in this article. The richest part of Ti element correlated direction to the andesitic unites. The developments in multifractal theory in special and their usage could provide a favorable ground for the stochastic simulation of geochemical distributions, and their understanding and interpretations, as well.

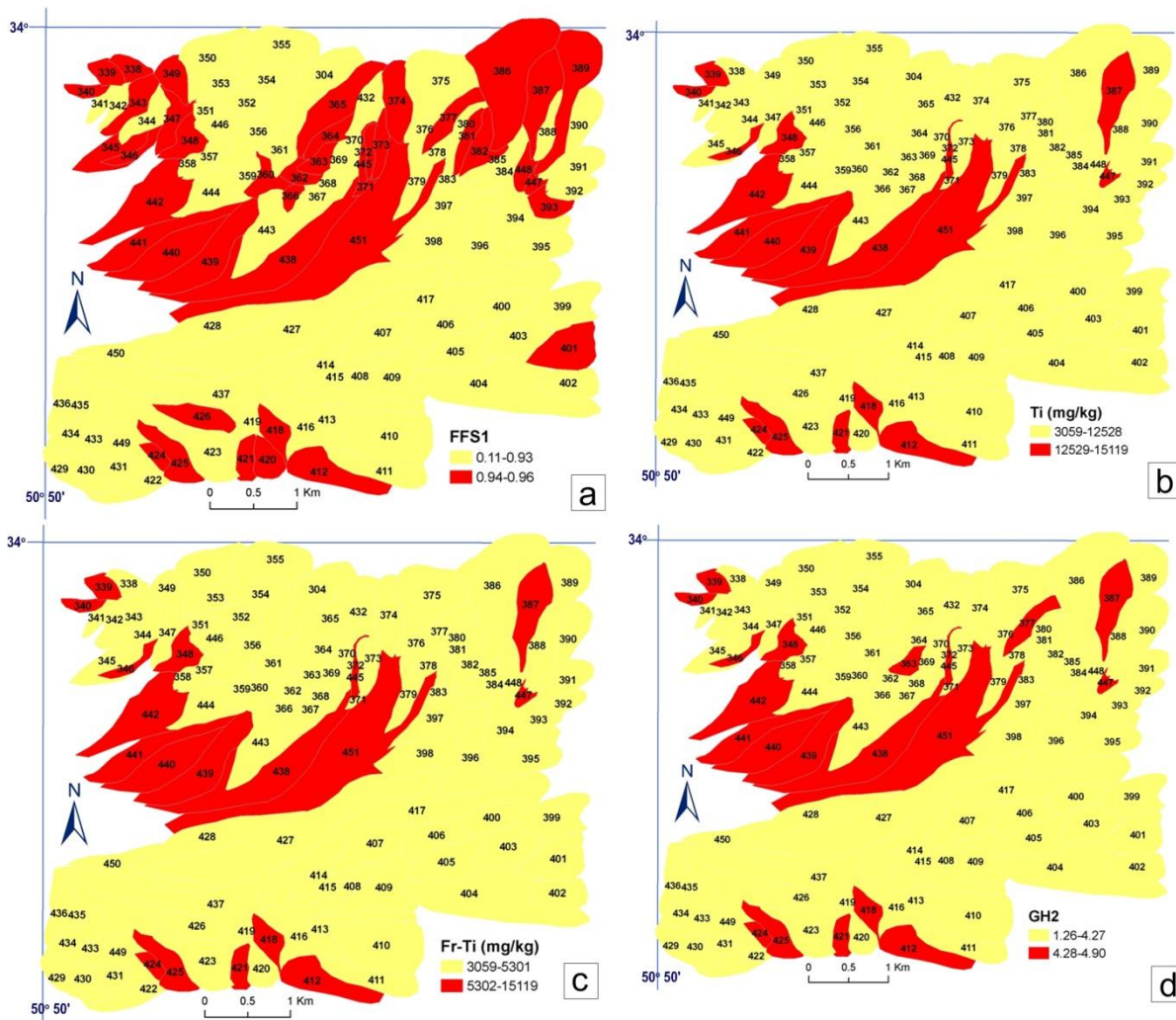


Fig.13. Target areas for (a); Ti delineated by means of 97.5% of fuzzy factor score (FFS1-Ti), (b); main concentration (Ti), (c); fractal method (Fr-Ti) and (d); geochemical halos of Ti (GH2).

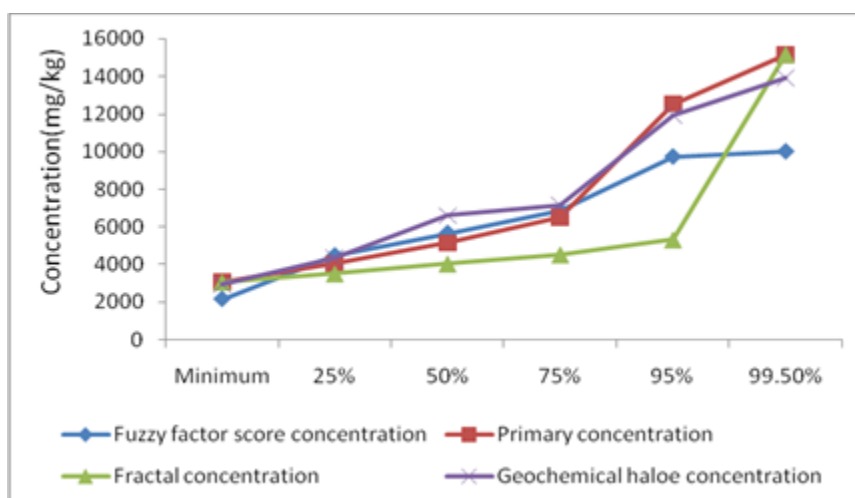


Fig.14. Targets delineated by means of different models of anomaly mapping for Ti.

## 5. Conclusions

Descriptive statistical studies conducted for stream sediments of the Delijan area show that most of elements have an asymmetric distribution. After ratio transformation and standardization, all elements achieve normal distribution. Results of stepwise factor and cluster analysis reveal that there are four factors or groups which are well correlated to each other. Factor 1 represents Co, Fe, Ti and V association, factor 2 related to Zn, Ba, Mn and Zr, factor 3 and factor 4 shows Ni, Cr and U, respectively, and the total variance of these factors to be 85.72%. Then, low valued elements (such as As, Cu, Pb, Au and Sr) omitted during three stepwise factor analysis. In order to outline the geochemical markers of mineralization-derived stream sediments more efficiently, various mapping techniques such as fuzzy factor score, geochemical halos and fractal model were used. In preparation of element distribution maps, the threshold value was computed using the multifractal model. This method can be considered as an alternative technique which is commonly used for the determination of background values. A comparison of anomaly maps and geology of the study area reveals that mineralization is closely related to the andesitic rocks in form of lava and dike with an Eocene age. Results of studies of heavy minerals showed that Ti value has been enriched in studied sediments. In addition, enrichment of other elements (based on lithology) suggests a multi-element association with mineralization in the area and should be further investigated in the next phase of mineral exploration.

## Acknowledgments

The authors thank from Mining Organization of Markazi Province for the results of elemental data. We also appreciate the comments of the anonymous reviewers.

## References

- [1] Shahabpour, J. (1994). Post-mineralization breccia dike from the Sar Cheshmeh porphyry copper deposit, Kerman, Iran. *Exploration and Mining Geology*, 3, 39–43.
- [2] Pazand, K., Hezarkhani, A. and Ataei, M. (2012). Using TOPSIS approaches for predictive porphyry Cu potential mapping: A case study in Ahar-Arasbaran area (NW, Iran). *Computers & Geosciences*, 49, 62–71.
- [3] Zheng, Y., Sun, X., Gao, S., Wang, C., Zhao, Z., Wu, S., Li, J. & Wu, X. (2014). Analysis of stream sediment data for exploring the Zhunuo porphyry Cu deposit, southern Tibet. *Journal of Geochemical Exploration*, 143, 19–30.
- [4] Carranza, E.J.M. (2009). Mapping of anomalies in continuous and discrete fields of Stream sediment geochemical landscapes. *Geochemistry: Exploration, Environment, Analysis*, 10, 171–187.
- [5] Carranza, E.J.M. (2010). Catchment basin modeling of stream sediment anomalies revisited incorporation of EDA and fractal analysis. *Geochemistry: Exploration, Environment, Analysis*, 10, 365–381.
- [6] Cheng, Q., Bonham-Carter, G.F., Wang, W., Zhang, S., Li, W. & Xia, Q. (2011). A spatial weighted principal component analysis for multi-element geochemical data for mapping locations of felsic intrusions in the Gejiu mineral district of Yunnan, China. *Computers and Geosciences*, 5, 662–669.
- [7] Grunsky, E.C. (2010). The interpretation of geochemical survey data. *Geochemistry: Exploration, Environment, Analysis*, 10, 27–74.

- [8] Zuo, R., Cheng, Q. & Agterberg, F.P. (2009a). Application of a hybrid method combining multilevel fuzzy comprehensive evaluation with asymmetric fuzzy relation analysis to mapping prospectivity. *Ore Geology Reviews*, 35, 101–108.
- [9] Zuo, R., Cheng, Q., Agterberg, F.P. & Xia, Q. (2009b). Application of singularity mapping technique to identification local anomalies using stream sediment geochemical data, a case study from Gangdese, Tibet, Western China. *Journal of Geochemical Exploration*, 101, 225–235.
- [10] Zuo, R. (2014). Identification of weak geochemical anomalies using robust neighborhood statistics coupled with GIS in covered areas. *Journal of Geochemical Exploration*, 136, 93–101.
- [11] Grunsky, E.C., Drew, L.J. & Sutphin, D.M. (2009). Process recognition in multi-element soil and stream-sediment geochemical data. *Applied Geochemistry*, 24, 1602–1616.
- [12] Sun, X., Deng, J., Gong, Q., Wang, Q., Yang, L. & Zhao, Z. (2009). Kohonen neural network and factor analysis based approach to geochemical data pattern recognition. *Journal of Geochemical Exploration*, 103, 6–16.
- [13] Yousefi, M., Kamkar-Rouhani, A. & Carranza, E.J.M. (2012). Geochemical Mineralization probability index (GMPI): A new approach to generate enhanced stream sediment geochemical evidential map for increasing probability of success in mineral potential mapping. *Journal of Geochemical Exploration*, 115, 24–35.
- [14] Yousefi, M., Carranza, E.J.M. & Kamkar-Rouhani, A. (2014). Weighted drainage catchment basin mapping of geochemical anomalies using stream sediment data for mineral potential modeling. *Journal of Geochemical Exploration*. 128, 88-96.
- [15] Harraz, Z.H., Hamdy, M.M. & El-Mamoney, M.H. (2012). Multi-element association analysis of stream sediment geochemistry data for predicting gold deposits in Barramiya gold mine, Eastern Desert, Egypt. *Journal of African Earth Sciences*, 68, 1–14.
- [16] Johnson, R. A. & Wichern, D.W. (2002). *Applied Multivariate Statistical Analysis*. Prentice Hall, Upper Saddle River, New Jersey, 513 p.
- [17] Cheng, Q., Agterberg, F.P. & Ballantyne, S.B. (1994). The separation of geochemical anomalies from background by fractal methods. *Journal of Geochemical Exploration*, 54, 109–130.
- [18] Cheng, Q. (2007). Mapping singularities with stream sediment geochemical data for prediction of undiscovered mineral deposits in Gejiu, Yunnan Province, China. *Ore Geology Reviews*, 32, 314–324.
- [19] Cheng, Q. & Agterberg, F. (2009). Singularity analysis of ore-mineral and toxic trace elements in stream sediments. *Computers and Geosciences*, 35, 234–244.
- [20] Cheng, Q., Xia, Q., Li, W., Zhang, S., Chen, Z., Zuo, R. & Wang, W. (2010). Density/area power-law models for separating multi scale anomalies of ore and toxic elements in stream sediments in Gejiu mineral district, Yunnan Province, China. *Biogeosciences*, 7, 3019–3025.
- [21] Zuo, R. (2011a). Decomposing of mixed pattern of arsenic using fractal model in Gangdese Belt, Tibet, China. *Applied Geochemistry*, 26, 271–273.
- [22] Zuo, R. & Xia, Q. (2009). Application fractal and multifractal methods to mapping prospectivity for metamorphosed sedimentary iron deposits using stream sediment geochemical data in eastern Hebei province, China. *Geochimica et Cosmochimica Acta*, 73, 1494–1541.
- [23] Hassanpour, Sh. & Afzal, P. (2013). Application of concentration-number (C-N) multifractal modelling for geochemical anomaly separation in Haftcheshmeh porphyry system, NW Iran. *Arabian Journal of Geosciences* 6, 957–970.
- [24] Heidari, M. Ghaderi, M. & Afzal, P. (2013). Delineating mineralized phases based on lithochemical data using multifractal model in Tuzlar epithermal Au-Ag (Cu) deposit, NW Iran. *Applied Geochemistry* 31, 119-132.
- [25] Afzal, P., Harati, H., Fadakar Alghalandis, Y. & Yasrebi, A.B. (2013). Application of spectrum-area fractal model to identify of geochemical anomalies based on soil data in Kahang porphyry-type Cu deposit, Iran. *Chemie der Erde* 73, 533– 543.
- [26] Alavi, M. (1994). Tectonic of Zagros orogenic belt of Iran new data and interpretations. *Tectonophysics*, 229, 211–238.
- [27] Pichab, K. (2011). Exploration studies of Au in Delijan. Report, Geological Organization of Iran, Delijan, 231 p.
- [28] Lahermo, P., Väänänen, P., Tavainen, T. & Salminen, R. (1996). *Environmental Geochemistry–Stream Waters and Sediments (III)*, Geochemical Atlas, Finland, Geological Survey of Finland, Espoo, 150 p.
- [29] Spadoni, M., Voltaggio, M. & Cavarretta, G. (2005). Recognition of areas of Anomalous concentration of potentially hazardous elements by means of a subcatchment-based discriminant analysis of stream sediments. *Journal of Geochemical Exploration*, 87, 83–91.
- [30] Spadoni, M. (2006). Geochemical mapping using a geomorphologic approach based on catchments. *Journal of Geochemical Exploration*, 90, 183–196.
- [31] Reimann, C. & Filzmoser, P. (2000). Normal and lognormal data distribution in geochemistry: death of a

myth, Consequences for the statistical treatment of geochemical and environmental data. *Environmental Geology*, 39, 1001–1014.

[32] Aitchison, J. (1986). *The statistical analysis of compositional data*. UK: Chapman and Hall, London, 416 p.

[33] Egozcue, J. J., Pawlowsky-Glahn, V., Mateu-Figueras, G. & Barceló-Vidal, C. (2003). Isometric logratio transformations for compositional data analysis. *Mathematical Geology*, 35, 279–300.

[34] Carranza, E.J.M. (2011). Analysis and mapping of geochemical anomalies using logratiotransformed stream sediment data with censored values. *Journal of Geochemical Exploration*, 110, 167–185.

[35] Jolliffe, T. (2002). *Principal Component Analysis*. Springer Verlag, New York, 488 p.

[36] Zuo, R. (2011). Identifying geochemical anomalies associated with Cu and Pb-Zn skarn mineralization using principal component analysis and spectrum-area fractal modeling in the Gandese Belt, Tibet (China). *Journal of Geochemical Exploration*, 111, 13–22.

[37] Afzal, P., Khakzad, A., Moarefvand, P., Rashidnejad Omran., N, Esfandiari, B. & Fadakar Alghalandis, Y. (2010). Geochemical anomaly separation by multifractal modeling in Kahang (Gor Gor) porphyry system, Central Iran. *Journal of Geochemical Exploration*, 104, 34–46.

[38] Xiao, F. & Chen, J. (2012). Fractal projection pursuit classification model applied to Geochemical survey data. *Computers & Geosciences*, 45, 75–81.

[39] Shamseddin Meigoony, M., Afzal, P., Gholinejad, M., Yasrebi, A.B. & Sadeghi, B. (2014). Delineation of geochemical anomalies using factor analysis and multifractal modeling based on stream sediments data in Sarajeh 1:100,000 sheet, Central Iran. *Arabian Journal of Geosciences*, 7, 5333–5343.

[40] Geranian, H., Mokhtari, A.R. & Cohen, D.R. (2013). A comparison of fractal methods and probability plots in identifying and mapping soil metal contamination near an active mining area, Iran. *Science of the Total Environment*, 463, 845–854.

[41] Wedepohl, K.H. (1995). The composition of the continental crust. *Geochim Cosmochim Acta*, 59, 1217–1232.

[42] Rudnick, R.L. & Gao, S. (2005). Composition of the Continental Crust. In: Holland, H.D., Turekian K.K. (eds), *Treatise on Geochemistry*, Vol. 3: The Crust, 3, 1-64.

[43] Kaiser, H.F. (1958). The varimax criterion for analytic rotation in factor analysis. *Psychometrika*, 23, 187-200.

[44] Cox, D.R. and Snell, E.J. (1989). *Analysis of Binary Data*. Chapman and Hall, London, 240 p.

[45] Beus, A.A. & Grigorian, S.V. (1977). In: Levinson A., A. (ed.), *Geochemical Exploration Methods for Mineral Deposits*, Applied Publishing Ltd., Moscow, 280 p.

[46] Reis, A.P., Sousa, A.J. & Cardoso- Fonseca, E. (2001). Soil geochemical prospecting for gold at Marrancos (Northern Portugal). *Journal of Geochemical Exploration*, 73, 1–10.